LWT - Food Science and Technology 152 (2021) 112261

Contents lists available at ScienceDirect

LWT

journal homepage: www.elsevier.com/locate/lwt

Water vapor sorption and permeability of sustainable alginate/collagen/SiO_2 composite films

Luís Marangoni Júnior [a,*], Renan Garcia da Silva [a,b], Roniérik Pioli Vieira [b], Rosa Maria Vercelino Alves [a]

[a] Packaging Technology Center, Institute of Food Technology, Campinas, São Paulo, Brazil
[b] Department of Bioprocess and Materials Engineering, School of Chemical Engineering, University of Campinas, Campinas, São Paulo, Brazil

ARTICLE INFO

Keywords:
Biopolymer
Food packaging
Moisture sorption

ABSTRACT

Films based on polysaccharides and proteins have been widely studied as possible substitutes for food packaging from fossil sources. However, its notorious sensitivity to water is still one of the primary drawbacks. In this study, sodium alginate (SA) and hydrolyzed collagen (HC) blend films containing SiO_2 nanoparticles were prepared to reduce the water sensitivity. The behavior of these films regarding water vapor sorption and permeability (WVP) was reported for nano-SiO_2 concentrations ranging from 2 to 10%. At each concentration evaluated, several classical mathematical models of moisture sorption isotherms were adjusted to identify the mechanisms of interactions between films and water. A reduction of approximately 8% in the film water content, and 30% reduction of WVP were observed for concentrations of nano-SiO_2 higher than 6%. In addition, it was exposed that the moisture sorption exhibited a type III isotherm behavior, suggesting reduced interactions between the polymeric matrix and water vapor at low water activity. Therefore, SA/HC/SiO_2 composite films could represent a simple, economical and sustainable alternative for packaging material with reduced sensitivity to water vapor.

1. Introduction

Bio-based polymers, such as proteins and carbohydrates, stand out as important renewable and biodegradable raw materials for sustainable food packaging applications (Júnior et al., 2021; Vianna et al., 2021). However, one of the key challenges for enabling a broad use of these polymers for this purpose remains their severe sensitivity to water vapor and poor mechanical properties (Marangoni Júnior et al., 2021). In this context, the formulation of blends using different biopolymers in parallel to obtaining composites becomes a powerful strategy in improving the properties for food packaging applications (Nur Hanani et al., 2014; Ramos et al., 2016; Xie et al., 2013; Youssef & El-Sayed, 2018). A vast number of biological sources demonstrate potential, but they still need to be extensively studied for their performance to be acceptable (Marangoni Júnior et al., 2020).

Obtained from brown algae, sodium alginate (SA) represents one of the most versatile polysaccharides in nature (Rahmani et al., 2017). Since SA is a biodegradable and non-toxic polymer, it has been extensively employed in the food and medical fields (Uyen et al., 2020; Venkatesan et al., 2015). In the food packaging sector, SA is well-known to be used successfully in the production of edible films (Senturk Parreidt et al., 2018). However, the SA fragility and high sensitivity to water remain the principal difficulties in its widespread food packaging applications (Hou et al., 2019). Thus, the development of SA-based films blended with other polysaccharides or proteins becomes the most simple and attractive strategy for improving properties (Yang et al., 2020). Among the numerous biopolymers, such as starch, chitosan, carrageenan, pectin, whey protein isolate and gelatin that are available for the formulation of blends with SA (Tavassoli-Kafrani et al., 2016), hydrolyzed collagen has been little explored.

Hydrolyzed collagen (HC) is a group of peptides that can be obtained by enzymatic action in an acid or alkaline environment, extracted from bovine, porcine and marine sources of native collagen (León-López et al., 2019). The HC average molar masses range from 3 to 6 kDa, which are considerably lower than the precursor native collagen (285–300 kDa). Hydrolysis affects not only the size of the peptides, but also the physicochemical properties (improvement in water solubility and odor, lower viscosity, among others) (Denis et al., 2008; Zhang et al., 2006). In addition, the composition and degree of collagen hydrolysis comprise factors that significantly increase functional properties, such as

* Corresponding author. Av. Brasil, 2880, CEP: 13070-178, Campinas, SP, Brazil.
E-mail address: marangoni.junior@hotmail.com (L. Marangoni Júnior).

https://doi.org/10.1016/j.lwt.2021.112261
Received 21 April 2021; Received in revised form 3 August 2021; Accepted 4 August 2021
Available online 5 August 2021

antioxidant capacity, antimicrobial activity and greater bioavailability (Li et al., 2013; Wang, Luo, et al., 2018; Wang, Luo, et al., 2018; Zhang et al., 2017). However, despite possessing such advantages over native collagen, HC is unable to form films by itself, being necessary to combine it with other biopolymers (Ramadass et al., 2014; Silvipriya et al., 2015).

In this context, SA/HC blends could be simple and economical alternatives in the manufacture of functional films for food packaging. The idea of using HC in the SA-based film formulation is to provide resulting material with peptides intrinsic and widely known functional properties. To enhance the physicochemical properties of these blends, nanoparticles inclusion appears as another easy and economically accessible strategy that can be used in parallel to the production of biopolymer blends. For example, nano-SiO_2 (SiO_2) has been extensively employed in this regard (Fabbri et al., 2006; Kavya et al., 2013; Salimi et al., 2017; Tabatabaei et al., 2018; Yang et al., 2016). The fundamental hypothesis of this work was that blends of SA and HC with different nano-SiO_2 contents could reduce the sensitivity to water vapor. That is, the higher the concentration of nanoparticles, the greater the barrier to water vapor and the lower the moisture content of the films.

Therefore, the aim of this study was to evaluate the effect of adding different proportions of nano-SiO_2 on the water vapor permeability and moisture sorption of SA/HC blend films in a broad range of relative humidity (0–95% RH). For this, the blend was preliminarily evaluated to identify the most proper proportion of SA and HC, which was used as a control sample for this study. Seven mathematical models of different sorption isotherms were adjusted to assist in the structure-properties correlation of sensitivity to water vapor. The importance of this work lies in the fact that it is a first description of interactions between SA/HC/SiO_2 blends and water vapor. Another novel aspect of this research is the identification nano-SiO_2 proportions thresholds to further reduce the water vapor permeability and moisture content. With this, we believe this work may be the starting point in the expansion of hydrolyzed collagen containing films studies, which are still scarce.

2. Material and methods

2.1. Material

The materials used in the preparation of the films were: sodium alginate (SA) (Dinâmica Química Contemporânea Ltda, Indaiatuba/SP, Brazil), hydrolyzed collagen (HC) (NaturalLife, São José do Rio Preto/SP, Brazil), glycerol (Dinâmica Química Contemporânea Ltda, Indaiatuba/SP, Brazil), and nano-SiO_2 (SiO_2) with average particle size of 12 nm (Evonik/Degussa Ltda, Americana/SP, Brazil).

2.2. Preparation of the films

The casting method was employed in the manufacture of sodium alginate/hydrolyzed collagen films with SiO_2 nanoparticles (SA/HC/SiO_2). Sodium alginate solutions (4% w/w) were prepared by dissolving the biopolymer in distilled water containing glycerol as a plasticizer (30% w/w, considering de sodium alginate mass as calculation basis), hydrolyzed collagen (10% w/w, considering sodium alginate mass as calculation basis), and different concentrations of SiO_2 nanoparticles were added (0, 2, 6, 8 and 10% w/w, considering sodium alginate mass as calculation basis). The proportion of HC used in this work was based on preliminary tests, in which several proportions were evaluated to identify the most homogeneous films. The samples were coded as SA/HC, SA/HC/2%SiO_2, SA/HC/6%SiO_2, SA/HC/8%SiO_2, and SA/HC/10%SiO_2, respectively. Film-forming solution was heated to 80 °C with stirring for 20 min. Subsequently, the final solution was treated in an ultrasound bath for 15 min, to ensure a homogeneous solution and elimination of bubbles. After this step, 50 g of film-forming solutions were poured into polystyrene Petri dishes (diameter 14 cm) and dried at 40 °C for 24 h in a forced air circulation oven (Ethik Technology, Vargem Grande Paulista/SP, Brazil). Finally, after removing the films from the plates, all the samples were stored in an air-conditioning chamber (Weiss Technik, Reiskirchen, Germany) at 25 °C and 75% relative humidity (RH), as a step prior to the characterization processes.

2.3. Thickness

The SA/HC/SiO_2 films thicknesses were determined in a micrometer with a measurement system composed of a flat granite base and dial indicator (Mitutoyo Co., Kawasaki-Shi, Japan), with 0.1 μm resolution, after conditioning, for 48 h, at 25 ± 2 °C and 75 ± 5% RH. The average thickness of each formulation sample was determined using five random points from five different replicates, according to the standard methodology (ISO-4593, 1993).

2.4. Moisture content

The moisture content (MC) of each sample was determined by gravimetry. After drying the film sample at 105 °C for 24 h, in an oven (Ethik Technology, Vargem Grande Paulista/SP, Brazil), mass loss was determined using an analytical balance (Mettler Toledo, Columbus, Ohio, USA) with resolution of 10^{-4} g. The MC values (%) were determined, using four repetitions for each sample analyzed, according to equation (1):

$$MC = \frac{w_i - w_f}{w_i} \times 100\ \% \quad (1)$$

in wich w_i and w_f are the initial and final weights of the sample, respectively.

2.5. Water vapor permeability

The water vapor transmission rate (WVTR) and water vapor permeability (WVP) were determined in triplicate using the gravimetric method of analysis, following the methodology (ASTM-E96/E96M, 2016). A capsule with a permeation area of 50 cm^2 containing anhydrous calcium chloride desiccant, and an analytical balance with resolution of 10^{-4} g (Mettler Toledo, Columbus, Ohio, USA) were used to determine WVTR and WVP. The test was performed at 25 °C and 75% RH in an air conditioning chamber (Weiss Technik, Reiskirchen, Germany). The WVTR (g m^{-2} day^{-1}) was determined from the slope of the curve "mass change vs. time". Finally, WVP (g m^{-1} s^{-1} Pa^{-1}) of the film was calculated according to equation (2):

$$WVP = \frac{WVTR \times e}{p_s \times RH_1} \quad (2)$$

in which e is the specimen average thickness (μm), p_s is the water vapor saturation pressure (23.756 mmHg at 25 °C), RH_1 is the relative humidity of the chamber (75% = factor 0.75), since the relative humidity inside the capsule is considered to be zero.

2.6. Determination of the moisture sorption isotherms

Gravimetric sorption measurements were determined for all samples using a controlled atmosphere Dynamic Vapor Sorption system (model DVS-002), Surface Measurements System (London, UK) at 25 °C. Only the adsorption test was performed, in which each sample was cut into pieces of ~0.5 × 0.5 cm and placed in a vacuum oven (45 °C) for 18 h. After that, the sample was placed in a desiccator to cool to room temperature (~20 min), and then a sample portion with a mass of ~50 mg was analyzed in the equipment. During the analysis, the sample was exposed to the following RH profile at 25 °C: 0.00, 10.56, 21.11, 31.67, 42.22, 52.78, 63.33, 73.89, 84.44, and 95% RH. The RH step lasted until reaching mass equilibrium. Moisture sorption of each sample at equilibrium was calculated as the gained water mass (grams) per grams of dry film at the range of relative humidity.

2.7. Modeling of moisture sorption isotherms

For each film sample, the experimental data were fitted to some classical mathematical models for moisture sorption predictions (Table 1). X_{eq} is the equilibrium moisture content in dry basis (d. b.), which is provided by g H_2O/g of dried solids, a_w is the water activity, and A, B, C, M_0, and K are constant parameters of the models. The determination of such constants used to fit the data was carried out employing the *Excel*® software. The generalized reduced gradient (GRG) method from the *Excel Solver* was performed to estimate the GAB and BET model parameters, by minimizing the Residual Standard Deviation (S_{res}) (Equation (3)) between experimental and predicted values. The other models were linearized and a straight line was adjusted, allowing the determination of parameters A and B from the angular and linear coefficients. In order to evaluate the goodness of the curve fitting, in all cases the determination coefficients (R^2) and Residual Standard Deviation (S_{res}) were provided. The models in which $R^2 > 0.98$ and $S_{res} < 0.2$ were considered as good fit.

$$S_{res} = \sqrt{\frac{\sum \left(Y_{exp} - Y_{sim}\right)^2}{n-2}} \quad (3)$$

which S_{res} is the Residual Standard Deviation, Y_{exp} is the experimental value, Y_{sim} is the predicted value (simulation) and "n" is number of experimental data.

2.8. Statistical analysis

The results were statistically evaluated by means of analysis of variance (ANOVA) and the Tukey test to compare the average results ($p < 0.05$).

3. Results and discussions

3.1. Thickness and moisture content

The thickness of the films ranged from 160.6 ± 40.2 to 195.0 ± 42.9 μm, as shown in Table 2. Concentrations up to 8% of nano-SiO_2 did not significantly influence ($p < 0.05$) the thickness of the films, when comparing to the control film (SA/HC). Similar results have been found in the literature for fish gelatin/k-carrageenan films added with 1–5% SiO_2 (Tabatabaei et al., 2018). The SA/HC/10%SiO_2 film showed the highest thickness value. However, the thickness of this film did not differ significantly ($p < 0.05$) from the SA/HC/2%SiO_2 and SA/HC/8%SiO_2 films. The increase in the thickness of the film, comparing to the control sample is attributed to the higher concentration of solids (10% SiO_2) in the polymeric matrix.

Table 2 shows there was a significative reduction in the films moisture content (MC) for nano-SiO_2 concentrations above 6%, comparing to the control sample. In addition, the films with concentrations of 6, 8 and 10% of SiO_2 did not present significant MC difference ($p < 0.05$) between them. The reduction in MC of the composite films is mainly influenced by the hydrogen bonds formed between SA, HC and nano-SiO_2 (Abdollahi et al., 2013). In addition, with the increase of SiO_2, the carboxyl and hydroxyl groups of SA can interact with the hydroxyl groups of nano-SiO_2, which leads to the formation of new hydrogen bonds. Consequently, it can cause strengthening of intermolecular interactions, with reductions in bonds with other molecules of water (Yang et al., 2018). This phenomenon of reduction in moisture content with the addition of nano-SiO_2 was observed by other authors in pullulan/-whey protein isolate films (Hassannia-Kolaee et al., 2016) and sodium alginate/polyvinyl alcohol (Yang et al., 2018). These preliminary results of moisture content determined by manual gravimetry are in line with what was observed in the moisture sorption tests using the DVS equipment. More details will be described in the subsequent sections.

Table 1
Mathematical models for moisture sorption predictions.

Model	Equation	Parameters
Guggenhiem-Anderson-Boer (GAB)	$X_{eq} = \frac{M_0 \times C \times K \times a_w}{(1 - K \times a_w)(1 - K \times a_w + C \times K \times a_w)}$	M_0, C, K
Brunauer-Emmitt-Teller (BET)	$X_{eq} = \frac{M_0 \times C \times a_w}{(1 - a_w)(1 + C \times a_w - a_w)}$	M_0, C
Smith	$X_{eq} = A + B \times ln(1 - a_w)$	A, B
Henderson	$X_{eq} = \left[\frac{-ln(1 - a_w)}{A}\right]^{\frac{1}{B}}$	A, B
Flory-Huggings	$X_{eq} = A \times \exp(B \times a_w)$	A, B
Oswin	$X_{eq} = A \times \left(\frac{a_w}{1 - a_w}\right)^B$	A, B
Halsey	$X_{eq} = \left[-\frac{A}{\ln(a_w)}\right]^{\frac{1}{B}}$	A, B

Table 2
Thickness and moisture content of the films of sodium alginate/hydrolyzed collagen/SiO_2.

Samples	Thickness (μm)	Moisture content (%)
SA/HC	160.6 ± 40.2^{b}	25.3 ± 1.6^{a}
SA/HC/2%SiO_2	178.9 ± 37.5^{ab}	25.9 ± 0.7^{a}
SA/HC/6%SiO_2	161.5 ± 35.1^{b}	23.1 ± 0.5^{b}
SA/HC/8%SiO_2	180.6 ± 36.2^{ab}	23.0 ± 0.9^{b}
SA/HC/10%SiO_2	195.0 ± 42.9^{a}	23.2 ± 0.3^{b}

The results are expressed as mean ± standard deviation.
[a, b, c] The averages of results followed by the same letter in the same column do not differ at the 95% confidence level ($p < 0.05$).

3.2. Water vapor permeability

The water vapor barrier property is an important parameter that should be improved for biopolymer-based films, since these compounds are well-known to possess high affinity to water. When biopolymer-based films are applied to food it is desirable that they minimize the exchange of moisture between the food and the environment, and vice-versa (Xu et al., 2020). The water vapor transmission rate (WVTR) and water vapor permeability (WVP) of the SA/HC control films were 1023.4 ± 121.9 g m^{-2} day^{-1} and 7.5 ± 0.3 × 10^{-10} g m^{-1} s^{-1} Pa^{-1}, respectively (Fig. 1). The addition of 2% nano-SiO_2 does not significantly influenced ($p < 0.05$) the WVTR and WVP values of the films. That is, the low nano-SiO_2 concentration did not improve the films water vapor barrier properties. A similar effect was found by Rane et al. (2014) in K-carrageenan films with 1.5% SiO_2 nanoparticles.

Conversely, comparing to the control and SA/HC/2%SiO_2 film samples, a significant reduction ($p < 0.05$) was observed in the WVTR and WVP, when concentration of 6–10% nano-SiO_2 were employed. The improvement in the water vapor barrier properties of films added with nano-SiO_2 is attributed to the formation of hydrogen bonds between the polymeric matrix and the oxygen atoms of the nanoparticles (Hassannia-Kolaee et al., 2016; Shahabi-Ghahfarrokhi et al., 2015), which can reduce the water solubility coefficient throughout the polymeric matrix. Moreover, the good dispersion of the SiO_2 nanoparticles filled the void spaces in the film, which makes the path tortuous and consequently hinders the diffusion of water molecules through the polymeric matrix (Kristo & Biliaderis, 2007; Priyadarshi et al., 2021).

3.3. Moisture sorption isotherms

Fig. 2 provides the moisture sorption isotherms for all formulations, with comparison of the profiles simulated by the mathematical models that presented the best fit. It was verified, from Fig. 2 (a), that the isotherms for films containing different concentrations of nano-SiO_2 exhibited a similar trend. The moisture content of the films gradually

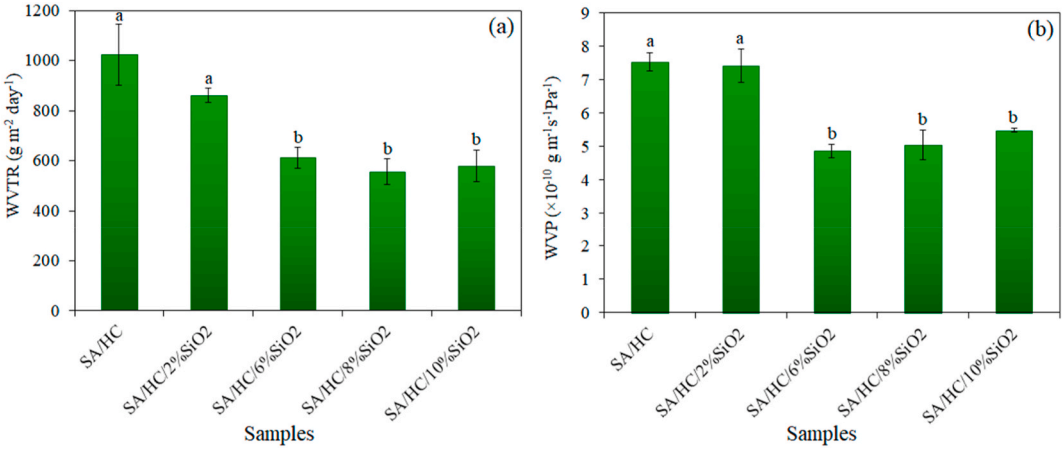

Fig. 1. Water vapor permeability of sodium alginate/hydrolyzed collagen/SiO_2 films.

increased linearly for a_w below 0.4, with remarkably low and virtually equivalent values for all samples. A sharp increase in the moisture content of the films only started to become noticeable for a_w values ranging from 0.4 to 0.95, with an exponential profile. According to Brunauer et al. this profile can be considered as a type III isotherm (Brunauer et al., 1940), which refers to a curvature of the convex isotherm towards the a_w axis throughout the range. In the case of the SA/HC/SiO_2 composite films, this behavior suggests that the attractive forces between adsorbed water vapor and film matrix (hydroxyls and carboxyl groups) are lower than the attractive forces between the water molecules in the liquid state. Sodium alginate, hydrolyzed collagen and nano-SiO_2 form composites with good compatibility, that is, intermolecular interactions are favored. As a result, there is a reduced availability of possible functional groups for adsorption of water molecules, explaining the observed behavior.

A type III isotherm profile similar to that reported in this study was identified for other pure alginate-based films (Olivas & Barbosa-Cánovas, 2008; Rhim, 2004), and for powdered cocona pulp microencapsulated with hydrolyzed collagen and maltodextrin blend (Vargas-Muñoz et al., 2020). This profile is repeated for alginate films using glycerol as plasticizer, in which the higher the proportion of glycerol the higher the equilibrium moisture content. Conversely, this behavior differs somewhat from the sigmoidal profile widely reported for other pure biopolymers and blend films, such as starch (Suppakul et al., 2013), chitosan (Rosa et al., 2010), among others (Galus & Lenart, 2013; Hazaveh et al., 2015; Xiao & Tong, 2013). It was observed that alginate films without plasticizer also tended to maintain a sigmoidal profile (Olivas & Barbosa-Cánovas, 2008).

Differences between the moisture values of films with different concentrations of nano-SiO_2 only started to be noticeable for $a_w > 0.6$. Fig. 2 (a) also illustrates the moisture content of the films tends to decrease with the increase in the concentration of nanoparticles. For example, for the highest value of a_w evaluated ($a_w = 0.95$), the film moisture decreased from 57 to 50% d. b., comparing the control and the film containing 10% of nano-SiO_2, respectively. Since the permeability could be calculated from water vapor diffusivity in the film matrix and the solubility coefficient, it appears that the reduction of this variable, even on a small scale, may have contributed to the inferior results of water vapor permeability obtained in this study. However, clearly the reduction in diffusivity due to the inclusion of obstacles (nanoparticles) throughout the matrix should remain the key factor for the significant permeability reductions observed previously in Fig. 1.

Seven mathematical models were fitted to the experimental data of this study. Fig. 2 (b)–(f) provides a comparison between each experimental point and the two most appropriate adjustments: GAB and Smith (considering the entire range of water activity - a_w). Table 3 provides the determined parameters for all models, with the values of R^2 and S_{res}. Although the GAB model had a proper fit in general, it is necessary to note that at low a_w values there were some considerable deviations. It is well-known this model is more suitable for values of a_w up to 0.9. In this way, as all experimental points in the a_w domain were considered, the mathematical method certainly converged to parameter values that met the entire range of values, sacrificing deviations at the beginning of the domain. As the values of experimental moisture content below $a_w = 0.2$ were practically zero, it was considered in this study that these initial deviations are acceptable. The BET model did not represent properly the moisture content values for $a_w > 0.4$, providing an unsatisfactory R^2 and corroborating with what has already been observed in the literature (Andrade et al., 2011). Other possible justifications for these deviations refer to the fact that a type III isotherm does not have a "knee point" as in the sigmoidal profiles, which means that there is no restricted multilayer formation (Nazreen et al., 2020).

Therefore, alternative models were expected for better reproduction of the experimental data. Smith's empirical model was developed to describe the final curved portion of the water sorption isotherm of high molecular weight polymers (Smith, 1947). Fig. 2 and parameters determined in Table 3 indicate that the experimental data were well reproduced over all a_w range. Mathematically, negative moisture content values were obtained with Smith's model at $a_w < 0.2$, which were considered to be zero to provide a physical meaning. It is significant to highlight that type III curve is equally known as the Flory-Huggins isotherm (Al-Muhtaseb et al., 2002; Nazreen et al., 2020), and this model was also evaluated in this study. Although it was the model with the most optimistic expectation, it was detected that there was a satisfactory reproduction for a_w values up to 0.7, being therefore not indicated in this case. Other models were also unsatisfactory to represent the entire a_w range.

4. Conclusion

Significant reductions were observed in the moisture content (MC), water vapor transmission rate (WVTR) and water vapor permeability (WVP) of the sodium alginate/hydrolyzed collagen films for nano-SiO_2 concentrations greater than 6%. Analysis of moisture sorption over a broad range of water activity (a_w) values reveled a type III isotherm behavior for all the film samples, suggesting the attractive forces between adsorbed water vapor and film matrix (hydroxyls and carboxyl groups) are lower than the attractive forces between the water molecules in the liquid state. As a general conclusion, the results indicated that sodium alginate, hydrolyzed collagen and nano-SiO_2 form composites films with good compatibility, reducing the availability of possible functional groups for water molecules adsorption. Therefore, the addition of nano-SiO_2 in blended films composed of sodium alginate and hydrolyzed collagen can be considered a simple, environmentally

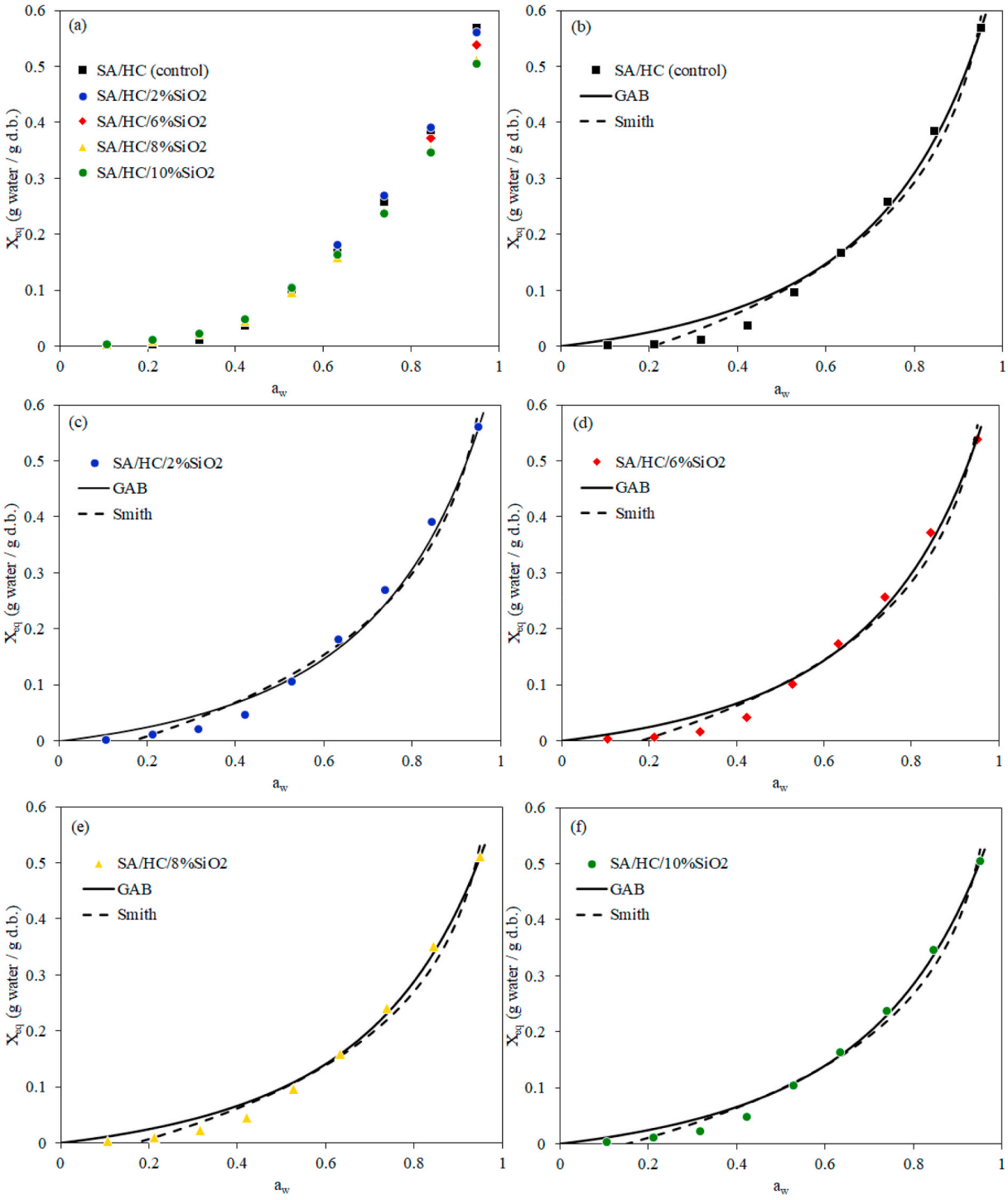

Fig. 2. Equilibrium moisture sorption isotherm of sodium alginate, hydrolyzed collagen and SiO_2 composites films (SA/HC/SiO_2) as a function of water activity (a_w) at 25 °C; (a) comparison between experimental data containing different nano-SiO_2 concentrations; and comparison between experimental data and the two best models fitted for (b) SA/HC, (c) SA/HC/2%SiO_2, (d) SA/HC/6%SiO_2, (e) SA/HC/8%SiO_2 and (f) SA/HC/10%SiO_2.

friendly and economical alternative for reducing the sensitivity to water vapor.

CRediT authorship contribution statement

Luís Marangoni Júnior: Conceptualization, Data curation, Formal analysis, Investigation, Methodology, Project administration, Writing – original draft, Writing – review & editing. **Renan Garcia da Silva:** Formal analysis, Investigation, Writing – review & editing. **Roniérik Pioli Vieira:** Conceptualization, Data curation, Formal analysis, Funding acquisition, Investigation, Methodology, Project administration, Resources, Supervision, Writing – original draft, Writing – review & editing. **Rosa Maria Vercelino Alves:** Conceptualization, Data curation, Formal analysis, Funding acquisition, Investigation, Methodology, Project administration, Resources, Supervision, Writing – review & editing.

Table 3
Parameters for the sorption equations used in this research.

Model parameters	SA/HC (control)	SA/HC/ 2%SiO_2	SA/HC/ 6%SiO_2	SA/HC/ 8%SiO_2	SA/HC/ 10%SiO_2
Guggenhiem – Anderson – Boer (GAB)					
M_0	0.574	0.574	0.572	0.581	0.581
C	0.238	0.238	0.238	0.240	0.240
K	0.706	0.703	0.697	0.684	0.681
R^2	0.995	0.993	0.993	0.997	0.997
S_{res}	0.148	0.147	0.145	0.124	0.117
Brunauer – Emmitt – Teller (BET)					
M_0	0.033	0.033	0.031	0.030	0.029
C	40.083	169.55	104.6	242.7	245.3
R^2	0.815	0.795	0.798	0.810	0.800
S_{res}	0.097	0.103	0.098	0.091	0.091
Smith					
A	−0.049	−0.038	−0.039	−0.035	−0.031
B	−0.214	−0.209	−0.201	−0.189	−0.186
R^2	0.985	0.984	0.984	0.987	0.988
S_{res}	0.026	0.026	0.026	0.021	0.020
Henderson					
A	2.982	3.062	3.349	3.659	3.641
B	0.493	0.551	0.573	0.620	0.624
R^2	0.883	0.899	0.910	0.935	0.934
S_{res}	0.170	0.154	0.112	0.0834	0.087
Flory-Huggings					
A	0.0012	0.0023	0.0023	0.0032	0.0034
B	7.237	6.361	6.227	5.733	5.684
R^2	0.917	0.932	0.937	0.959	0.956
S_{res}	0.190	0.157	0.127	0.093	0.098
Oswin					
A	0.038	0.052	0.049	0.054	0.055
B	1.299	1.153	1.120	1.036	1.027
R^2	0.735	0.751	0.763	0.796	0.796
S_{res}	0.452	0.376	0.308	0.242	0.245
Halsey					
A	0.082	0.078	0.072	0.065	0.065
B	0.613	0.695	0.708	0.765	0.773
R^2	0.686	0.699	0.707	0.739	0.739
S_{res}	0.606	0.479	0.416	0.328	0.326

Declaration of competing interest

The authors declare that they have no known competing financial interests or personal relationships that could have appeared to influence the work reported in this paper.

Acknowledgments

The authors acknowledge the National Council for Scientific and Technological Development (CNPq). This study was partly financed by the Coordination for the Improvement of Higher Education Personnel – Brazil (CAPES) – Financial Code 001.

References

Abdollahi, M., Alboofetileh, M., Rezaei, M., & Behrooz, R. (2013). Comparing physico-mechanical and thermal properties of alginate nanocomposite films reinforced with organic and/or inorganic nanofillers. *Food Hydrocolloids, 32*, 416–424. https://doi.org/10.1016/j.foodhyd.2013.02.006

Al-Muhtaseb, A. H., McMinn, W. A. M., & Magee, T. R. A. (2002). Moisture sorption isotherm characteristics of food products: A review. *Food and Bioproducts Processing, 80*, 118–128. https://doi.org/10.1205/09603080252938753

Andrade, R. D., Lemus, R., & Pérez, C. (2011). Models of sorption isotherms for food: Uses and limitations. *VITAE, Rev. LA Fac. QUÍMICA Farm., 18*, 325–334.

ASTM-E96/E96M. (2016). *Standard test methods for water vapor transmission of materials* (p. 14p). West Conshohocken.

Brunauer, S., Deming, L. S., Deming, W. E., & Teller, E. (1940). On a theory of the van der Waals adsorption of gases. *Journal of the American Chemical Society, 62*, 1723–1732. https://doi.org/10.1021/ja01864a025

Denis, A., Brambati, N., Dessauvages, B., Guedj, S., Ridoux, C., Meffre, N., & Autier, C. (2008). Molecular weight determination of hydrolyzed collagens. *Food Hydrocolloids, 22*, 989–994. https://doi.org/10.1016/j.foodhyd.2007.05.016

Fabbri, P., Singh, B., Leterrier, Y., Månson, J.-A. E., Messori, M., & Pilati, F. (2006). Cohesive and adhesive properties of polycaprolactone/silica hybrid coatings on poly (methyl methacrylate) substrates. *Surface and Coatings Technology, 200*, 6706–6712. https://doi.org/10.1016/j.surfcoat.2005.10.003

Galus, S., & Lenart, A. (2013). Development and characterization of composite edible films based on sodium alginate and pectin. *Journal of Food Engineering, 115*, 459–465. https://doi.org/10.1016/j.jfoodeng.2012.03.006

Hassannia-Kolaee, M., Khodaiyan, F., Pourahmad, R., & Shahabi-Ghahfarrokhi, I. (2016). Development of ecofriendly bionanocomposite: Whey protein isolate/pullulan films with nano-SiO2. *International Journal of Biological Macromolecules, 86*, 139–144. https://doi.org/10.1016/j.ijbiomac.2016.01.032

Hazaveh, P., Mohammadi Nafchi, A., & Abbaspour, H. (2015). The effects of sugars on moisture sorption isotherm and functional properties of cold water fish gelatin films. *International Journal of Biological Macromolecules, 79*, 370–376. https://doi.org/10.1016/j.ijbiomac.2015.05.008

Hou, X., Xue, Z., Xia, Y., Qin, Y., Zhang, G., Liu, H., & Li, K. (2019). Effect of SiO2 nanoparticle on the physical and chemical properties of eco-friendly agar/sodium alginate nanocomposite film. *International Journal of Biological Macromolecules, 125*, 1289–1298. https://doi.org/10.1016/j.ijbiomac.2018.09.109

ISO-4593. (1993). *Plastics: Film and sheeting determination of thickness by mechanical scanning*. Switzerland (p. 2p).

Júnior, L. M., da Silva, R. G., Anjos, C. A. R., Vieira, R. P., & Alves, R. M. V. (2021). Effect of low concentrations of SiO2 nanoparticles on the physical and chemical properties of sodium alginate-based films. *Carbohydrate Polymers*. , Article 118286. https://doi.org/10.1016/j.carbpol.2021.118286

Kavya, K. C., Jayakumar, R., Nair, S., & Chennazhi, K. P. (2013). Fabrication and characterization of chitosan/gelatin/nSiO2 composite scaffold for bone tissue engineering. *International Journal of Biological Macromolecules, 59*, 255–263. https://doi.org/10.1016/j.ijbiomac.2013.04.023

Kristo, E., & Biliaderis, C. G. (2007). Physical properties of starch nanocrystal-reinforced pullulan films. *Carbohydrate Polymers, 68*, 146–158. https://doi.org/10.1016/j.carbpol.2006.07.021

León-López, A., Morales-Peñaloza, A., Martínez-Juárez, V. M., Vargas-Torres, A., Zeugolis, D. I., & Aguirre-Álvarez, G. (2019). Hydrolyzed collagen—sources and applications. *Molecules, 24*(22), 4031. https://doi.org/10.3390/molecules24224031

Li, Z., Wang, B., Chi, C., Gong, Y., Luo, H., & Ding, G. (2013). Influence of average molecular weight on antioxidant and functional properties of cartilage collagen hydrolysates from Sphyrna lewini, Dasyatis akjei and Raja porosa. *Food Research International, 51*, 283–293. https://doi.org/10.1016/j.foodres.2012.12.031

Marangoni Júnior, L., Vieira, R. P., & Anjos, C. A. R. (2020). Kefiran-based films: Fundamental concepts, formulation strategies and properties. *Carbohydrate Polymers, 246*, Article 116609. https://doi.org/10.1016/j.carbpol.2020.116609

Marangoni Júnior, L., Vieira, R. P., Jamróz, E., & Anjos, C. A. R. (2021). Furcellaran: An innovative biopolymer in the production of films and coatings. *Carbohydrate Polymers, 252*, Article 117221. https://doi.org/10.1016/j.carbpol.2020.117221

Nazreen, A. Z., Jai, J., Abdulbari Ali, S., & Mohamed Manshor, N. (2020). Moisture adsorption isotherm model for edible food film packaging – a review. *Sci. Res. J., 17*, 222–245. https://doi.org/10.24191/srj.v17i2.10160

Nur Hanani, Z. A., Roos, Y. H., & Kerry, J. P. (2014). Use and application of gelatin as potential biodegradable packaging materials for food products. *International Journal of Biological Macromolecules, 71*, 94–102. https://doi.org/10.1016/j.ijbiomac.2014.04.027

Olivas, G. I., & Barbosa-Cánovas, G. V. (2008). Alginate–calcium films: Water vapor permeability and mechanical properties as affected by plasticizer and relative humidity. *Lebensmittel-Wissenschaft und -Technologie- Food Science and Technology, 41*, 359–366. https://doi.org/10.1016/j.lwt.2007.02.015

Priyadarshi, R., Kim, H. J., & Rhim, J. W. (2021). Effect of sulfur nanoparticles on properties of alginate-based films for active food packaging applications. *Food Hydrocolloids, 110*, Article 106155. https://doi.org/10.1016/j.foodhyd.2020.106155

Rahmani, B., Hosseini, H., Khani, M., Farhoodi, M., Honarvar, Z., Feizollahi, E., Shokri, B., & Shojaee-Aliabadi, S. (2017). Development and characterisation of chitosan or alginate-coated low density polyethylene films containing Satureja hortensis extract. *International Journal of Biological Macromolecules, 105*, 121–130. https://doi.org/10.1016/j.ijbiomac.2017.07.002

Ramadass, S. K., Perumal, S., Gopinath, A., Nisal, A., Subramanian, S., & Madhan, B. (2014). Sol–gel assisted fabrication of collagen hydrolysate composite scaffold: A novel therapeutic alternative to the traditional collagen scaffold. *ACS Applied Materials & Interfaces, 6*, 15015–15025. https://doi.org/10.1021/am502948g

Ramos, M., Valdés, A., Beltrán, A., & Garrigós, M. C. (2016). Gelatin-based films and coatings for food packaging applications. *Coatings, 6*(4), 41. https://doi.org/10.3390/coatings6040041

Rane, L. R., Savadekar, N. R., Kadam, P. G., & Mhaske, S. T. (2014). Preparation and characterization of K-Carrageenan/Nanosilica biocomposite film, 2014 *Journal of Materials*, 1–8. https://doi.org/10.1155/2014/736271.

Rhim, J.-W. (2004). Physical and mechanical properties of water resistant sodium alginate films. *Lebensmittel-Wissenschaft und -Technologie- Food Science and Technology, 37*, 323–330. https://doi.org/10.1016/j.lwt.2003.09.008

Rosa, G. S., Moraes, M. A., & Pinto, L. A. A. (2010). Moisture sorption properties of chitosan. *Lebensmittel-Wissenschaft und -Technologie- Food Science and Technology, 43*, 415–420. https://doi.org/10.1016/j.lwt.2009.09.003

Salimi, F., Tahmasobi, K., Karami, C., & Jahangiri, A. (2017). Preparation of modified nano-SiO2 by bismuth and iron as a novel remover of methylene blue from water solution. *J. Mex. Chem. Soc., 61*, 250–259. https://doi.org/10.29356/jmcs.v61i3.351

Senturk Parreidt, T., Müller, K., & Schmid, M. (2018). Alginate-based edible films and coatings for food packaging applications. *Foods, 7*(10), 170. https://doi.org/10.3390/foods7100170

Shahabi-Ghahfarrokhi, I., Khodaiyan, F., & Mousavi, M. (2015). Preparation of UV-protective kefiran/nano-ZnO nanocomposites : Physical and mechanical properties. *International Journal of Biological Macromolecules, 72*, 41–46. https://doi.org/10.1016/j.ijbiomac.2014.07.047

Silvipriya, K. S., Krishna Kumar, K., Bhat, A. R., Dinesh Kumar, B., John, A., & Lakshmanan, P. (2015). Collagen: Animal sources and biomedical application. *Journal of Applied Pharmaceutical Science, 5*, 123–127. https://doi.org/10.7324/JAPS.2015.50322

Smith, S. E. (1947). The sorption of water vapor by high polymers. *Journal of the American Chemical Society, 69*, 646–651. https://doi.org/10.1021/ja01195a053

Suppakul, P., Chalernsook, B., Ratisuthawat, B., Prapasitthi, S., & Munchukangwan, N. (2013). Empirical modeling of moisture sorption characteristics and mechanical and barrier properties of cassava flour film and their relation to plasticizing–antiplasticizing effects. *Lebensmittel-Wissenschaft und -Technologie- Food Science and Technology, 50*, 290–297. https://doi.org/10.1016/j.lwt.2012.05.013

Tabatabaei, R. H., Jafari, S. M., Mirzaei, H., Nafchi, A. M., & Dehnad, D. (2018). Preparation and characterization of nano-SiO2 reinforced gelatin-k-carrageenan biocomposites. *International Journal of Biological Macromolecules, 111*, 1091–1099. https://doi.org/10.1016/j.ijbiomac.2018.01.116

Tavassoli-Kafrani, E., Shekarchizadeh, H., & Masoudpour-Behabadi, M. (2016). Development of edible films and coatings from alginates and carrageenans. *Carbohydrate Polymers, 137*, 360–374. https://doi.org/10.1016/j.carbpol.2015.10.074

Uyen, N. T. T., Hamid, Z. A. A., Tram, N. X. T., & Ahmad, N. (2020). Fabrication of alginate microspheres for drug delivery: A review. *International Journal of Biological Macromolecules, 153*, 1035–1046. https://doi.org/10.1016/j.ijbiomac.2019.10.233

Vargas-Muñoz, D. P., de Oliveira, L. A. N., da Silva, L. C., Godoy, H. T., & Kurozawa, L. E. (2020). Storage stability of 5-caffeoylquinic acid in powdered cocona pulp microencapsulated with hydrolyzed collagen and maltodextrin blend. *Food Research International, 137*, Article 109652. https://doi.org/10.1016/j.foodres.2020.109652

Venkatesan, J., Bhatnagar, I., Manivasagan, P., Kang, K.-H., & Kim, S.-K. (2015). Alginate composites for bone tissue engineering: A review. *International Journal of Biological Macromolecules, 72*, 269–281. https://doi.org/10.1016/j.ijbiomac.2014.07.008

Vianna, T. C., Marinho, C. O., Júnior, L. M., Ibrahim, S. A., & Vieira, R. P. (2021). Essential oils as additives in active starch-based food packaging films: A review. *International Journal of Biological Macromolecules, 182*, 1803–1819. https://doi.org/10.1016/j.ijbiomac.2021.05.170

Wang, L., Jiang, Y., Wang, X., Zhou, J., Cui, H., Xu, W., He, Y., Ma, H., & Gao, R. (2018). Effect of oral administration of collagen hydrolysates from Nile tilapia on the chronologically aged skin. *J. Funct. Foods, 44*, 112–117. https://doi.org/10.1016/j.jff.2018.03.005

Wang, J., Luo, D., Liang, M., Zhang, T., Yin, X., Zhang, Y., Yang, X., & Liu, W. (2018). Spectrum-effect relationships between high-performance liquid chromatography (HPLC) fingerprints and the antioxidant and anti-inflammatory activities of collagen peptides. *Mol, 23*(12), 3257. https://doi.org/10.3390/molecules23123257

Xiao, Q., & Tong, Q. (2013). Thermodynamic properties of moisture sorption in pullulan–sodium alginate based edible films. *Food Research International, 54*, 1605–1612. https://doi.org/10.1016/j.foodres.2013.09.019

Xie, F., Pollet, E., Halley, P. J., & Avérous, L. (2013). Starch-based nano-biocomposites. *Progress in Polymer Science, 38*, 1590–1628. https://doi.org/10.1016/j.progpolymsci.2013.05.002

Xu, L., Zhang, B., Qin, Y., Li, F., Yang, S., Lu, P., Wang, L., & Fan, J. (2020). Preparation and characterization of antifungal coating films composed of sodium alginate and cyclolipopeptides produced by Bacillus subtilis. *International Journal of Biological Macromolecules, 143*, 602–609. https://doi.org/10.1016/j.ijbiomac.2019.12.051

Yang, M., Shi, J., & Xia, Y. (2018). Effect of SiO2, PVA and glycerol concentrations on chemical and mechanical properties of alginate-based films. *International Journal of Biological Macromolecules, 107*, 2686–2694. https://doi.org/10.1016/j.ijbiomac.2017.10.162

Yang, M., Xia, Y., Wang, Y., Zhao, X., Xue, Z., Quan, F., Geng, C., & Zhao, Z. (2016). Preparation and property investigation of crosslinked alginate/silicon dioxide nanocomposite films. *Journal of Applied Polymer Science, 133*, 1–9. https://doi.org/10.1002/app.43489

Yang, L., Yang, J., Qin, X., Kan, J., Zeng, F., & Zhong, J. (2020). Ternary composite films with simultaneously enhanced strength and ductility: Effects of sodium alginate-gelatin weight ratio and graphene oxide content. *International Journal of Biological Macromolecules, 156*, 494–503. https://doi.org/10.1016/j.ijbiomac.2020.04.057

Youssef, A. M., & El-Sayed, S. M. (2018). Bionanocomposites materials for food packaging applications: Concepts and future outlook. *Carbohydrate Polymers, 193*, 19–27. https://doi.org/10.1016/j.carbpol.2018.03.088

Zhang, G., Sun, A., Li, W., Liu, T., & Su, Z. (2006). Mass spectrometric analysis of enzymatic digestion of denatured collagen for identification of collagen type. *Journal of Chromatography A, 1114*, 274–277. https://doi.org/10.1016/j.chroma.2006.03.039

Zhang, Y., Zhang, Y., Liu, X., Huang, L., Chen, Z., & Cheng, J. (2017). Influence of hydrolysis behaviour and microfluidisation on the functionality and structural properties of collagen hydrolysates. *Food Chemistry, 227*, 211–218. https://doi.org/10.1016/j.foodchem.2017.01.049